

The *desynaptic* (*dy*) and *desynaptic1* (*dsy1*) mutations in maize (*Zea mays* L.) cause distinct telomere-misplacement phenotypes during meiotic prophase

Hank W. Bass¹, Stefano J. Bordoli and Eric M. Foss

Department of Biological Science, Florida State University, Tallahassee, FL 32306-4370, USA

Received 5 August 2002; Accepted 12 September 2002

Abstract

During meiotic prophase, telomeres actively attach themselves to the nuclear envelope and cluster in an arrangement called the bouquet. The bouquet is unique to meiosis, highly conserved, and thought to facilitate homologous chromosome synapsis. Analysis of three-dimensional fluorescence *in situ* hybridization (3-D FISH) image data has been employed to characterize the bouquet in fixed pollen mother cells of maize (*Zea mays* L.). In order to examine the function of the bouquet further, several meiotic mutants were screened for telomeric defects using 3-D FISH as an assay. Two mutants, *desynaptic* (*dy*) and *desynaptic1* (*dsy1*), were found to exhibit novel telomere-misplacement phenotypes. In both cases, the telomere-associated mutant phenotypes occurred prior to what was previously reported as the earliest affected stage. Three alleles of the *desynaptic1* mutation (*dsy1-1*, *dsy1-9101*, and *dsy1-9307*) resulted in a partial bouquet phenotype at the zygotene stage of meiotic prophase. By contrast, *dy* nuclei contained apparently normal bouquets, but then resulted in a premature intranuclear localization of telomeres at the pachytene stage, when telomeres normally disperse but remain attached to the nuclear envelope. The *dsy1* mutation is known to impair the fidelity and progression of homologous synapsis, whereas the *dy* mutation is known to reduce recombination rates. If the telomere misplacements are primary defects of these mutants, then these data would be consistent with the hypothesis that meiotic telomeres have at least two separable functions, one involving proper homologous chromosome synapsis at the bouquet stage and another involving post-bouquet cross-over control.

Key words: Bouquet, chromosome, desynaptic, meiosis, nuclear envelope, nucleus, recombination, synapsis, telomere.

Introduction

Meiosis in higher plants involves a pair of specialized cell divisions that are essential for the production of gametes or gamete-producing cells (John, 1990). The meiosis-specific two-by-two pairing of homologous chromosomes ensures subsequent chromosome disjunction and segregation, which reduce the genome to the haploid state. Homologous chromosome synapsis and meiotic recombination occur during meiotic prophase (of the first division) and are prerequisites for the reductive division. The molecular, biochemical, and biophysical activities that occur during meiotic prophase have been extensively studied in many experimental systems (Zickler and Kleckner, 1998, 1999). Classic and recent studies from maize (*Zea mays* L.), arabidopsis (*Arabidopsis thaliana*), and other members of the plant kingdom have provided major contributions to knowledge of meiosis and sexual reproduction (Dawe, 1998, see also Caryl *et al.*, 2003; Schwarzacher, 2003).

Synapsis of homologous chromosomes is a hallmark of meiotic prophase, and it usually coincides with the presence of the bouquet, a specialized nuclear structure in which telomeres are clustered on the nuclear envelope (Dernburg *et al.*, 1995; Scherthan, 2001). The bouquet stage occurs in early meiotic prophase, is widely conserved in nature, and is believed to play some role in synapsis or recombination or both (Hiraoka, 1952; Moens *et al.*, 1989; Chikashige *et al.*, 1994; Scherthan *et al.*, 1994; Bass *et al.*, 1997; Trelles-Sticken *et al.*, 1999).

¹ To whom correspondence should be addressed. Fax: +1 850 644 0481. E-mail: bass@bio.fsu.edu

Three-dimensional epifluorescence microscopy has been used with fixed meiotic nuclei from maize to elucidate the timing and nature of meiotic telomere dynamics (Dawe *et al.*, 1994; Bass *et al.*, 1997, 2000; Carlton and Cande, 2002). In normal (wild-type) maize, telomeres cluster *de novo* at the leptotene–zygotene transition, coincident with the initial pairing of homologous chromosomes (Bass *et al.*, 2000). In the present study, 3-D telomere FISH was used to screen a collection of meiotic mutants with defective pairing or synapsis phenotypes (Curtis and Doyle, 1991). New results from the analysis of two different desynaptic mutants suggest that telomere mislocalization at different stages of meiotic prophase can be associated with different types of meiotic defects.

Materials and methods

Plant materials and fixation of pollen mother cells

The growth, harvest, and formaldehyde fixation of whole anthers in ‘meiocyte Buffer A’ was carried out as previously described for the 3-D acrylamide FISH method of Bass *et al.* (1997). Maize lines carrying mutant alleles of the *desynaptic* gene (*dy*, Stock U540B) or the *desynaptic1* gene (*dysl1*, Stock U640B) are available from Maize Genetics Cooperation—Stock Center (University of Illinois, Urbana, IL; <http://w3.ag.uiuc.edu/maize-coop/mgc-home.html>). The desynaptic mutant *dy* was obtained (from CG Williams) in 1997, propagated in the homozygous mutant form (*dy/dy*), designated *dy-CW97*, and grown in the greenhouse for these studies. The *dysl1* mutants (obtained from IN Golubovskaya) are male-sterile and propagated as self-fertilized heterozygotes. Siblings from self-fertilized heterozygotes segregate 3:1 for normal:desynaptic. Greenhouse-grown plants are scored as normal or desynaptic by inspection of post-meiotic anthers; mutant anthers lack filled pollen grains. The three alleles of *dysl1* used in this study (*dysl1-1*, *dysl1-9101*, and *dysl1-9307*) are described by Golubovskaya *et al.* (1997).

Acrylamide FISH and three-dimensional image collection

Fluorescent oligonucleotides were synthesized and used to stain telomeres with the probe MTLF (5′-FITC-CCCTAAACCCTAAACCCTAAACCCTAAA-3′) or the 5S rDNA loci with the probe ELMO-R (5′-ROX-GTCACCCATCCTAGTACTAC-3′, Genset Oligos, La Jolla, CA) as previously described (Bass *et al.*, 1997, 2000). After the FISH procedure, cells were counterstained with DAPI. For data collection, each optical section was imaged with three different filter sets for selective detection of DAPI (for detecting DNA and chromatin), FITC (for detecting telomere probe signals), and rhodamine (for detecting the 5S rDNA probe signals). Then the focal plane was moved 0.2 μm, and the three images collected again. Typically, 60–100 optical sections were used to image a single cell or cluster of cells, resulting in a 3-wavelength 3-D data set. Images were recorded with an Olympus IMT-2 wide-field microscope and an oil-immersion lens (60× NA 1.4 PlanApo, Olympus) with 1.5× magnification (Hiraoka *et al.*, 1991). The raw data were subjected to deblurring restoration by 3-D iterative deconvolution (Delta Vision; Applied Precision, Issaquah, WA). The resulting data sets were then cropped around individual whole nuclei prior to 3-D modelling and spatial analysis. For figure presentation, the images were slightly adjusted for brightness and contrast with linear scaling between the minimum (black) and maximum (white) pixel intensity setting. Through-focus projections were made under the ‘display maximum intensity’ option, which

was determined to provide the best view of the structures being imaged. Representative examples of the 3-D data sets from *dysl1* and *dy* are available online as movie files with one section per frame.

Spatial analysis of telomere positions

Individual nuclei were modelled and real-space measurements were made for an assessment of the proximity of the telomere FISH signals to the nuclear periphery. The 3-D modelling of nuclear edges and telomere positions was carried out with the Priism software set (IVE3.3, from DA Agard and JW Sedat; University of California, San Francisco, CA). Briefly, individual nuclei consisting of a series of optical sections were interactively modelled in each section with the EditPolygon program, which traced the edges of the nucleus in the DAPI image. The telomere positions were marked by the PickPoints program. The polygon series were connected into solid surface objects by the VolumeBuilder program. For each nucleus, the ‘3-D Real’ measurements from VolumeBuilder provided the shortest distance between each telomere and the nuclear periphery. Distances greater than 1.0 μm from the nuclear periphery were referred to as ‘not on the nuclear envelope’, as explained in the results.

Results

The patterns of telomere localization in normal (wild-type) maize

The timing of telomere clustering during the zygotene stage of meiotic prophase has been observed and described for nearly a century, yet relatively few experiments have demonstrated a clear cause-and-effect relationship between meiotic telomere behaviour and any of the major hallmark processes of meiotic prophase, homologue pairing, synapsis, formation of the synaptonemal complex, recombination, or chiasmata formation. Recently, a clear picture has emerged regarding changing distribution of telomeres as a function of progression through meiotic prophase. The current study was based on the assumption that meiotic telomeres play a direct role in one or more of these essential processes of meiotic prophase. This assumption provided the basis for the prediction that genetic disruption of meiotic telomere functions would prevent proper homologue pairing and disjunction, resulting in sterility or reduced fertility. Because the telomere clustering is unique to meiotic prophase, some meiosis-specific gene products should exist that, if disrupted by mutation, would give rise to desynaptic or asynaptic phenotypes. Thus, genetic disruption of telomere function would in some cases produce both telomere-misplacement phenotypes and desynaptic phenotypes.

A collection of maize meiotic mutants was screened by 3-D telomere FISH in search of just such mutants with the ultimate goal of molecular cloning of genes with meiotic telomere functions. For comparison, the normal telomere localization and nuclear morphology observed for maize pollen mother cell meiocytes, based on previously published work (Dawe *et al.*, 1994; summarized in Fig. 9 of Bass *et al.*, 1997, 2000; Carlton and Cande, 2002), is described below. At premeiotic interphase, telomeres are

dispersed throughout the nuclear volume, and the two nucleoli are fused as one large centralized nucleolus. The single, enlarged nature of the nucleolus persists throughout meiotic prophase. At the leptotene stage, the first stage of meiotic prophase, chromatin condensation is evident, and telomeres are still distributed throughout the nuclear volume but excluded from the region occupied by the nucleolus. Late in the leptotene stage, telomeres move to the nuclear periphery and cluster into the bouquet formation (Bass *et al.*, 1997). At the leptotene–zygotene transition stage, the telomeres form a relatively tight cluster and are all located in less than one-half of the nucleus. Occasionally, a couple of telomere FISH signals are not in the bouquet, presumably because of linkage to the nucleolus-organizing region, which is near the end the short arm of chromosome 6. The normally spherical knobs, blocks of heterochromatin found on some maize chromosomes, become elongated at this leptotene–zygotene transition stage (referred to as prezygotene in Dawe *et al.*, 1994). Throughout all of zygotene, the telomere cluster of the bouquet is present. At early pachytene, after synapsis is completed, the bouquet persists. At some point in middle pachytene, the telomere cluster disperses, and telomeres remain at the nuclear periphery. After pachytene, chromosomes continue to condense and contract, and the telomeres no longer remain intimately associated with the nuclear envelope. Maize has a diploid chromosome complement of $2n=2x=20$. At the end of a successful meiotic prophase, each nucleus should contain 10 bivalents with an average of one chiasma per chromosome arm.

The dsy1 mutation results in a partial bouquet phenotype

The *dsy1* mutation causes complete male sterility and nearly complete female sterility and must be propagated in the heterozygous form (Golubovskaya *et al.*, 1997). The meiosis-specific mutation exhibits incomplete pairing as the primary cytological abnormality; the earliest affected stage is the pachytene (Curtis and Doyle, 1991). 3-D telomere FISH was used to investigate three different alleles of *dsy1* (see Materials and methods), and representative nuclei are shown in Fig. 1.

Each row of panels presented in Fig. 1 contains images from a single *dsy1* nucleus. The first three images are through-focus projections of the three separate wavelengths (see Materials and methods and supplemental data). The DAPI channel images reveal the chromatin fibre morphology that is used to determine staging as previously summarized (Bass *et al.*, 1997). The fluorescein channel images (FITC, from the FITC-labelled probe MTLF) reveal the positions of individual telomeres, which appear as small discrete spots. The rhodamine channel images (RHOD, from the ROX-labelled probe ELMO-R) reveal the positions the 5S rDNA loci. Normally, two 5S rDNA signals are present per nucleus, one for each homologue.

The replicated sister chromatids are not usually resolved for the telomere or 5S rDNA signals, presumably because of the cohesion that holds sister chromatids together along their long axes throughout meiotic prophase. The last image in each row shows a projection of a 3-D model that was interactively built (see Materials and methods) for the nucleus in that same row. The models preserve the real-space coordinates and can be subjected to mathematical distance analyses. They are presented in order to show more clearly the distribution of the telomeres. During data analysis the models can be quickly rotated on screen and viewed from any angle or as stereo pairs. This method significantly facilitates comprehension of the relative positions of the structures within the 3-D reconstructions. The models portray the nuclear periphery in purple, the telomere FISH signals as small yellow spheres, and the 5S rDNA signals as red cubes.

Representative nuclei from homozygous *dsy1* meiocytes are presented in Fig. 1A–F. Several examples from early prophase (Fig. 1A–D) illustrate the telomere-misplacement phenotype that was discovered from this study. The telomere-misplacement phenotype of *dsy1* was observed at early prophase, during the bouquet stage, and can best be described as a partial bouquet. The majority of *dsy1* data was collected from the *dsy1-9307* plants, but both *dsy1-1* and *dsy1-9101* mutants also exhibited this partial-bouquet telomere-misplacement phenotype. Many of the telomere FISH signals did appear to be clustered, but several telomeres (typically 2–8 signals) per nucleus did not colocalize with the bouquet (indicated by white arrows, Fig. 1A–D). These observations are in contrast to those from normal maize, in which all but one or two of the telomeres colocalize with the bouquet in early prophase (Bass *et al.*, 1997).

At middle prophase in *dsy1* mutants (Fig. 1E), chromosome fibre thickness typical of the pachytene stage was observed, although fibres of zygotene stage-type thickness were sometimes evident in some optical sections. For the example shown (Fig. 1E), the 5S rDNA FISH signal, which always stains very brightly, is present in only one location indicative of homologous synapsis for that locus. Not all cells showed 5S rDNA pairing, however, as is clear from the well-separated 5S rDNA FISH signals (yellow arrows, Fig. 1F) in the late-prophase example. The appearance of thin fibres at pachytene and the failure of the 5S rDNA loci to pair are consistent with observations from the analysis of chromosome spreads from *dsy1* (Golubovskaya *et al.*, 1997), which revealed non-homologous and incomplete synapsis. These summary observations were based on inspection ($n > 100$), 3-D data collection ($n > 50$), and 3-D modelling ($n = 15$) of multiple *dsy1* nuclei. The partial-bouquet telomere-misplacement phenotype occurred at a stage earlier than any previously reported cytological defect for *dsy1*.

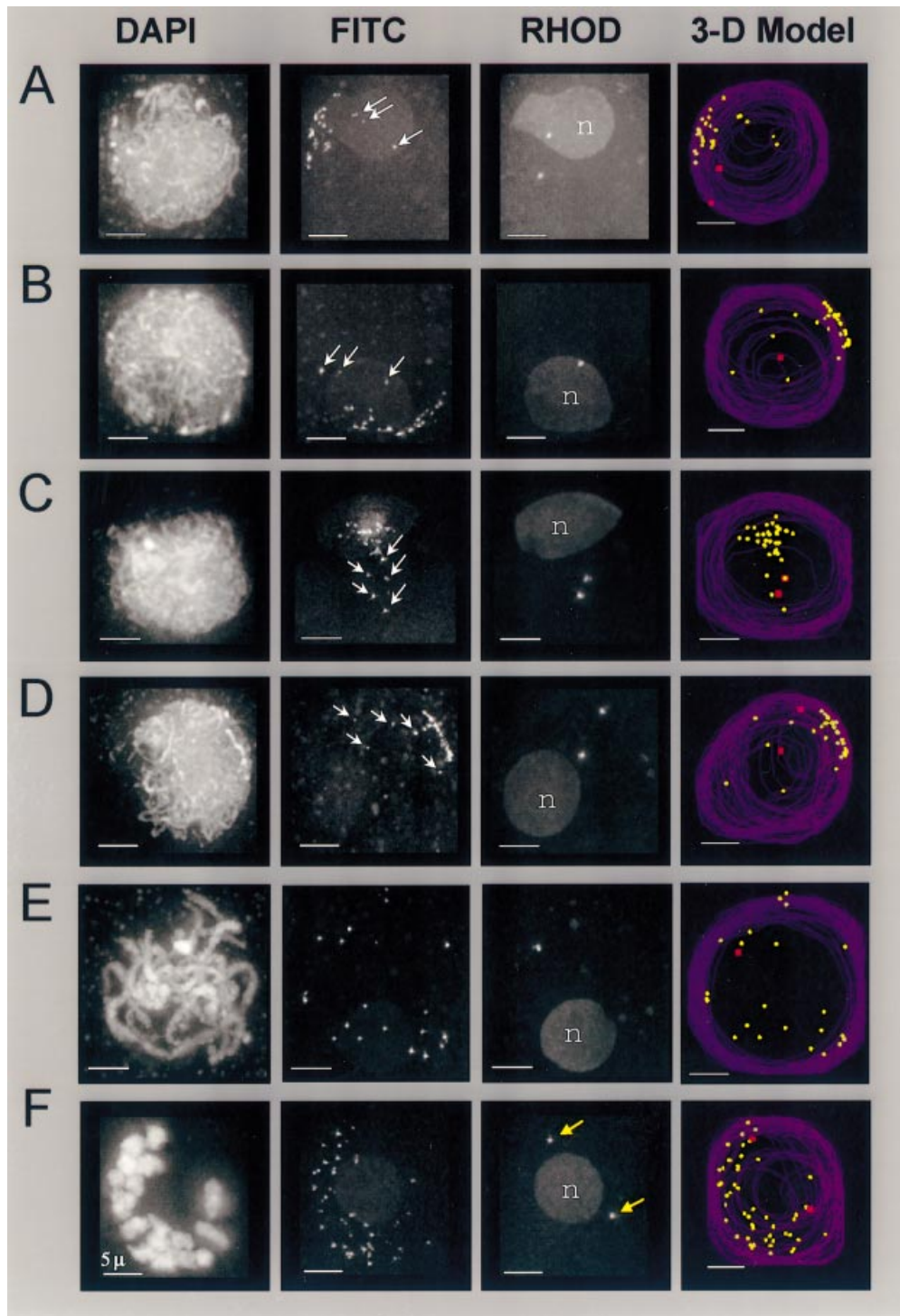


Fig. 1. Telomere-misplacement phenotype of *desynaptic1* (*dys1*). Through-focus projections of individual nuclei (A–F) are shown for each wavelength (DAPI, FITC, and RHOD (rhodamine)). Images in each row are from a single representative nucleus; a projection of a 3-D model is shown at the right. The positions of aberrant telomeres (white arrows), 5S rDNA FISH signals (yellow arrows), and the nucleolus (n) are indicated. Some examples of the *dys1* 3-D data are available online. All scale bars are 5 μ m.

dy results premature release of pachytene-stage telomeres from the nuclear envelope

dy results in reduced fertility, but can be propagated and analysed in the homozygous mutant form (Nelson and

Clary, 1952). The meiosis-specific mutation exhibits incomplete pairing as the primary cytological abnormality; the stage affected earliest is diplotene (Curtis and Doyle, 1991). *dy* is reported to disrupt the maintenance of chiasmata (Maguire, 1978), and genetic and cytogenetic

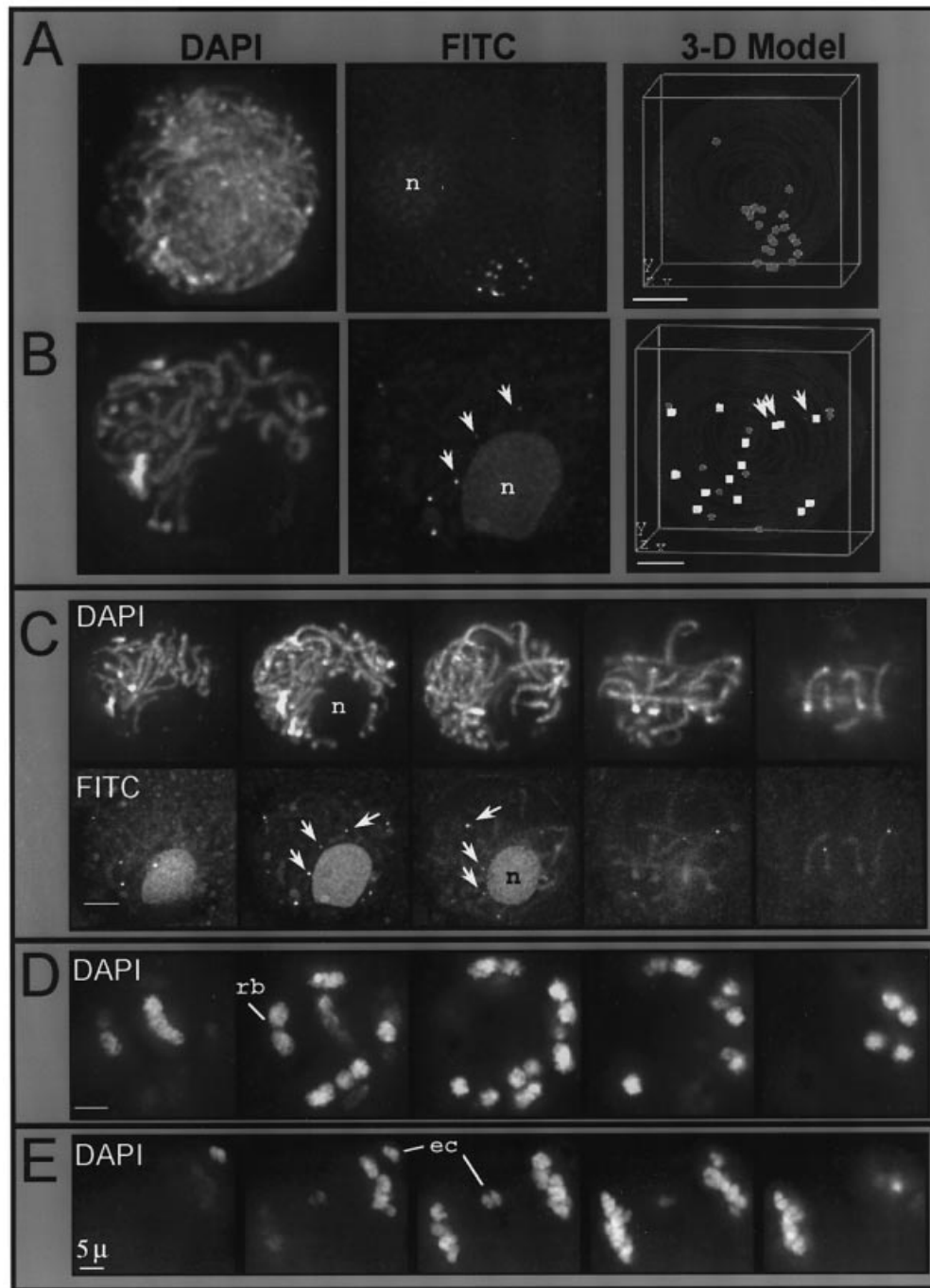


Fig. 2. Telomere-misplacement phenotype of *desynaptic* (*dy*). Early prophase (A) and middle prophase (B) nuclei show normal and aberrant telomere positions, respectively. The wavelength is indicated at the top, and the nuclei in (A) and (B) show a projection of the central 6 μm of each nucleus (not an entire through-focus projection). The 3-D model projection at the right is for the entire nucleus; telomeres at the periphery are shown as gray spheres (all of the telomeres in (A) are at the periphery), and telomeres not at the periphery (see Methods) are shown as white cubes (B). (C–E) Sequential projections through individual nuclei with the wavelength indicated in the upper left (DAPI or FITC). The positions of aberrant telomeres (white arrows), the nucleolus (n), an open-arm rod bivalent (rb), and chromosome excluded from the poles (ec) are indicated. The apparent stages are (A) zygotene; (B) pachytene; (C) pachytene (same nucleus as in B); (D) diplotene/diakinesis; (E) telophase. Some examples of the *dy* 3-D data are available online. All scale bars are 5 μm .

analyses indicate that it may be a recombination modifier gene (Ji *et al.*, 1999). The 3-D telomere FISH assay was used to screen for early prophase defects as described above, and the results are summarized in Fig. 2.

At early prophase, *dy* meiocytes appear to have normal bouquets (Fig. 1A), but at middle prophase, during pachytene, a major telomere-misplacement phenotype was observed (Fig. 2B, C). Namely, at pachytene, the

majority of telomere FISH signals were inside the nucleus (white arrows, Fig. 2B, C), rather than at the periphery. The 3-D models were used to determine the proportion of telomeres that were at the nuclear periphery in early and middle prophase. At early prophase in *dy*, nearly all of the telomere signals were at the nuclear periphery (defined here as less than 1 μm from the nuclear periphery), but at pachytene, a dramatic and unexpected internalization of telomeres signals was observed (white arrows and white cubes in Fig. 2B). For better representation of the spatial arrangements of telomeres and chromosomes in individual nuclei, Fig. 2 shows sequential projections (each representing 1/5 of the nucleus, see figure legend). The telomere FISH signals from the nucleus shown in Fig. 2C indicate that many telomeres are well within the inner space of the nucleus (white arrows). This aberrant pattern contrasts with that of wild-type cells, in which most of the telomeres are at the nuclear periphery in the pachytene stage. In late prophase, rod bivalents (rb, Fig. 2D), a typical feature of the mutant *dy*, can be observed. Figure 2E shows a cell at telophase of the first division. Although most of the chromosomes in this example have successfully segregated to one of the two poles (best seen in the lower left and upper right regions of the third and fourth projections), at least two chromosomes are excluded from the poles (indicated by 'ec'). Such configurations are typical of non-bivalent chromosomes.

The chromosome fibre morphology is the single best criterion for staging, and the acrylamide FISH technique generally preserves the structure and integrity of the sample. The mutants affect the chromosome morphology, however, and thereby make the exact staging inherently more problematic. Even so, a progression of chromosome condensation and contraction in the mutant meiocytes is clearly shown. To avoid the conundrum of whether a meiotic mutant with incomplete synapsis can ever truly be at pachytene (defined as complete synapsis), the percentage of telomeres at the nuclear periphery was determined as a function of the number of fibres in a cross-section. The number of fibres decreases with developmental stage in meiotic prophase. In normal meiocytes, most telomeres remained peripheral even in pachytene, which has about 5–12 fibres in cross-section. The persistent localization of telomeres at the periphery in pachytene, even after dispersal of the bouquet, is due to the end-on attachment of meiotic chromosomes to the nuclear envelope (Mogensen, 1977). In *dy*, however, the relocation of telomeres from nuclear periphery to the nuclear interior occurred at mid-prophase stages that resembled pachytene according to cross-sectional fibre number (Table 1). Mutant *dy* nuclei with 6–10 fibres (resembling the pachytene stage, e.g. Fig. 2C) always exhibited more internalized telomeres than expected. The summary observations for *dy* were based on inspection ($n > 100$), 3-D data collection ($n=20$), and 3-D modelling ($n=11$) of

Table 1. Telomere locations and fibre numbers in *dy* for several modelled 3-D data sets

Genotype	Fibre number	Stage	Peripheral telomeres
normal	12–20	Zygotene	90–100%
normal	5–12	Pachytene	80–100%
normal	0–5	Diplotene/Diakinesis	20–90%
<i>dy/dy</i>	17	Zygotene-like	100%
<i>dy/dy</i>	14	Zygotene-like	100%
<i>dy/dy</i>	10	Early-pachytene-like	62%
<i>dy/dy</i>	10	Early-pachytene-like	23%
<i>dy/dy</i>	9	Middle-pachytene-like	42%
<i>dy/dy</i>	8	Middle-pachytene-like	17%
<i>dy/dy</i>	8	Middle-pachytene-like	53%
<i>dy/dy</i>	7	Late-pachytene-like	44%
<i>dy/dy</i>	6	Late-pachytene-like	39%
<i>dy/dy</i>	2	Diakinesis	19%
<i>dy/dy</i>	0	Diakinesis	75%

multiple nuclei. This apparent premature detachment from the nuclear envelope occurred at a stage earlier than any previously reported cytological defect for *dy*.

Discussion

The application of molecular cytology was used to discover new aspects of desynaptic mutants. The *dsyl* mutants were found to exhibit a partial-bouquet telomere-misplacement phenotype. By contrast, *dy* mutants formed apparently normal bouquets, but then seemed to be defective for the maintenance of telomere-nuclear envelope interactions during middle prophase. Thus the mutant screen was informative and suggests that the normal alleles for these genes may encode products that directly or indirectly control meiotic telomere functions. Alternatively, the telomere-misplacement phenotypes could be unrelated to the primary genetic lesions; either or both might comprise only one aspect of a pleiotropic mutation. Not all mutations that affect meiotic chromosome segregation show telomere defects, however. Telomere FISH analyses of three other meiotic mutants (data not shown) indicate that mutations in some desynaptic genes (*desynaptic2*) do not disrupt meiotic telomere behavior, whereas other meiosis-specific mutations (*ameiotic-prophase arrest1* and *absence of first division*) result in a loss of the bouquet altogether as a downstream effect of an earlier cytological defect (HW Bass, WZ Cande, unpublished observations). Ultimately, the isolation and analysis of genes with meiotic telomere functions will help to clarify the degree to which the phenotypes reported here have a primary or causal role in the failure of synapsis.

The timing of telomere clustering described here is similar to that described for humans and many other organisms (for review see Scherthan, 2001), but several

interesting variations are well-documented for other plants. In hexaploid wheat, telomeres cluster earlier than in maize, and evidence suggests that centromere interactions at premeiotic interphase mediate some aspects of the homology search (Martinez-Perez *et al.*, 1999). In *Arabidopsis*, telomeres appear to cluster during meiotic prophase, but instead of clustering on the nuclear envelope, they associate on the nucleolus prior to homologous synapsis (Armstrong *et al.*, 2001). Major advances in the molecular and cytological analysis of meiosis in *Arabidopsis* have been made in recent years (Ross *et al.*, 1996; Fransz *et al.*, 1998). An increasing number of highly conserved meiotic genes have been identified in *Arabidopsis* through sequence analysis and transposon tagging strategies. Many of these conserved genes have functions related to the DNA metabolism associated with homologous chromosome synapsis, recombination, or sister chromatid cohesion (Caryl *et al.*, 2003; Schwarzacher, 2003). An intriguing question remains about the extent to which the nucleolus-associated telomere behavior in *Arabidopsis* is related, functionally and mechanistically, to the nuclear-envelope-associated telomere behaviour in other species.

In fission yeast (*S. pombe*), mutations in the *TAZI/LOT2* gene disrupt meiotic telomere clustering and result in reduced recombination and decreased sporulation. This mutation provided the first clear causal evidence that telomeres do in fact play essential and direct roles in meiosis (Cooper *et al.*, 1998; Nimmo *et al.*, 1998; Hiraoka *et al.*, 2000). Genetic disruption of the *taz1* telomere-binding protein causes meiotic as well as vegetative telomere defects. The results presented here are consistent with the possibility that *dysl1* is mutated for a telomeric protein gene, but the sterility of *dysl1* precludes an analysis of somatic telomeres over several generations. The *dy* mutation on the other hand has been propagated for many generations without any apparent progressive defect in normal growth of the plant. It is therefore unlikely that the normal allele of the *dy* gene is required for maintenance of somatic telomere integrity.

In conclusion, the current work provides evidence that telomere FISH screening of known mutants can uncover new aspects related to processes that occur during meiotic prophase. The purpose of this approach was to identify bouquet or bouquet-related mutants, as part of a larger goal of better understanding the structure–function relationships that operate at the prophase of the first meiotic division. In both cases, new information was obtained that should be useful for sorting out the timing and complexities of events that take place in the nucleus during meiotic prophase in a typical diploid multicellular organism.

Note: The supplementary information mentioned in this paper can be accessed from the online version of this

article, on the *Journal of Experimental Botany* website (at www.jxb.oupjournals.org).

Acknowledgements

We thank IN Golubovskaya and C Williams for providing genetic stocks, WZ Cande for helpful discussions, and C Marian and R Swofford for critical reading of the manuscript and assistance with production of the online movie data. This work was supported by the National Science Foundation (HWB; MCB-0091095), the Florida State University Research Foundation Program Enhancement Grant (HWB), and a JR Fisher Fellowship (SJB) from the American Cancer Society, Florida Division.

References

- Armstrong SJ, Franklin FC, Jones GH. 2001. Nucleolus-associated telomere clustering and pairing precede meiotic chromosome synapsis in *Arabidopsis thaliana*. *Journal of Cell Science* **114**, 4207–4217.
- Bass HW, Marshall WF, Sedat JW, Agard DA, Cande WZ. 1997. Telomeres cluster *de novo* before the initiation of synapsis: a three-dimensional spatial analysis of telomere positions before and during meiotic prophase. *Journal of Cell Biology* **137**, 5–18.
- Bass HW, Riera-Lizarazu O, Ananiev EV, Bordoli SJ, Rines HW, Phillips RL, Sedat JW, Agard DA, Cande WZ. 2000. Evidence for the coincident initiation of homolog pairing and synapsis during the telomere-clustering (bouquet) stage of meiotic prophase. *Journal of Cell Science* **113**, 1033–1042.
- Carlton PM, Cande WZ. 2002. Telomeres act autonomously in maize to organize the meiotic bouquet from a semipolarized chromosome orientation. *Journal of Cell Biology* **157**, 231–242.
- Caryl AP, Jones GH, Franklin FCH. 2003. Dissecting plant meiosis using *Arabidopsis thaliana* mutants. *Journal of Experimental Botany* **54**, 25–38.
- Chikashige Y, Ding D-Q, Funabiki H, Haraguchi T, Mashiko S, Yanagida M, Hiraoka Y. 1994. Telomere-led premeiotic chromosome movement in fission yeast. *Science* **264**, 270–273.
- Cooper JP, Watanabe Y, Nurse P. 1998. Fission yeast *Taz1* protein is required for meiotic telomere clustering and recombination. *Nature* **392**, 828–831.
- Curtis CA, Doyle GG. 1991. Double meiotic mutants of maize: implications for the genetic regulation of meiosis. *Journal of Heredity* **82**, 156–163.
- Dawe RK. 1998. Meiotic chromosome organization and segregation in plants. *Annual Review of Plant Physiology and Plant Molecular Biology* **49**, 371–395.
- Dawe RK, Sedat JW, Agard DA, Cande WZ. 1994. Meiotic chromosome pairing in maize is associated with a novel chromatin organization. *Cell* **76**, 901–912.
- Dernburg AF, Sedat JW, Cande WZ, Bass HW. 1995. Cytology of telomeres. In: Blackburn EH, Greider CW, ed. *Telomeres*. Plainview, New York: Cold Spring Harbor Laboratory Press, 295–338.
- Fransz P, Armstrong S, Alonso-Blanco C, Fischer TC, Torres-Ruiz RA, Jones G. 1998. Cytogenetics for the model system *Arabidopsis thaliana*. *The Plant Journal* **13**, 867–876.
- Golubovskaya IN, Grebennikova ZK, Auger DL, Sheridan WF. 1997. The maize *desynaptic 1* mutation disrupts meiotic chromosome synapsis. *Developmental Genetics* **21**, 146–159.
- Hiraoka T. 1952. Observational and experimental studies of meiosis with special reference to the bouquet stage. XIV. Some considerations on a probable mechanism of the bouquet formation. *Cytologia* **17**, 292–299.

- Hiraoka Y, Chen H, Sedat JW, Agard DA.** 1991. Three-dimensional fluorescence microscopy for the analysis of spatial arrangement of chromosomes. *Acta Histochemica et Cytochemica* **24**, 357–366.
- Hiraoka Y, Ding DQ, Yamamoto A, Tsutsumi C, Chikashige Y.** 2000. Characterization of fission yeast meiotic mutants based on live observation of meiotic prophase nuclear movement. *Chromosoma* **109**, 103–109.
- Ji Y, Stelly DM, De Donato M, Goodman MM, Williams CG.** 1999. A candidate recombination modifier gene for *Zea mays* L. *Genetics* **151**, 821–830.
- John B.** 1990. *Meiosis*. New York: Cambridge University Press.
- Maguire M.** 1978. Evidence for separate genetic control of crossing over and chiasma maintenance in maize. *Chromosoma* **65**, 173–183.
- Martinez-Perez E, Shaw P, Reader S, Aragon-Alcaide L, Miller T, Moore G.** 1999. Homologous chromosome pairing in wheat. *Journal of Cell Science* **112**, 1761–1769.
- Moens PB, Bernelot-Moens C, Spyropoulos B.** 1989. Chromosome core attachment to meiotic nuclear envelope regulates synapsis in *Chloealtis* (Orthoptera). *Genome* **32**, 601–610.
- Mogensen HL.** 1977. Ultrastructural analysis of female pachynema and the relationship between synaptonemal complex length and crossing-over in *Zea mays*. *Carlsberg Research Communications* **42**, 475–497.
- Nelson OE, Clary GB.** 1952. Genetic control of semisterility in maize. *Journal of Heredity* **43**, 205–210.
- Nimmo ER, Pidoux AL, Perry PE, Allshire RC.** 1998. Defective meiosis in telomere-silencing mutants of *Schizosaccharomyces pombe*. *Nature* **392**, 825–828.
- Ross KJ, Fransz P, Jones GH.** 1996. A light microscopic atlas of meiosis in *Arabidopsis thaliana*. *Chromosome Research* **4**, 507–516.
- Scherthan H.** 2001. A bouquet makes ends meet. *Nature Review of Molecular and Cellular Biology* **2**, 621–627.
- Scherthan H, Bahler J, Kohli J.** 1994. Dynamics of chromosome organization and pairing during meiotic prophase in fission yeast. *Journal of Cell Biology* **127**, 273–285.
- Schwarzacher G.** 2003. Meiosis recombination and chromosomes: a review of gene isolation and fluorescent *in situ* hybridization data in plants. *Journal of Experimental Botany* **54**, 11–23.
- Trelles-Sticken E, Loidl J, Scherthan H.** 1999. Bouquet formation in budding yeast: initiation of recombination is not required for meiotic telomere clustering. *Journal of Cell Science* **112**, 651–658.
- Zickler D, Kleckner N.** 1998. The leptotene–zygotene transition of meiosis. *Annual Review of Genetics* **32**, 619–697.
- Zickler D, Kleckner N.** 1999. Meiotic chromosomes: integrating structure and function. *Annual Review of Genetics* **33**, 603–754.